THE JOURNAL OF PHYSICAL CHEMISTRY B

 VOLUME 106, NUMBER 4, JANUARY 31, 2002

LETTERS

Coherent Excitation of Vibrational Modes in Gold Nanorods

Gregory V. Hartland*,† and Min Hu

Department of Chemistry and Biochemistry, University of Notre Dame, 251 Nieuwland Science Hall, Notre Dame, Indiana 46556-5670

Orla Wilson and Paul Mulvaney‡

School of Chemistry, The University of Melbourne, Victoria, 3010, Australia

John E. Sader§

Department of Mathematics and Statistics, The University of Melbourne, Victoria, 3010, Australia

Received: October 18, 2001

The acoustic vibrational modes of Au nanorods with aspect ratios between 2 and 5 have been investigated by time-resolved laser spectroscopy. The results show that laser excitation launches a coherent vibrational motion that has a period that depends linearly on the length of the rod. Due to polydispersity in the samples, the measured period also depends on the probe wavelength (i.e., different probe wavelengths interrogate different length rods). Analysis of the data provides information about the size distribution of the sample and the homogeneous line width of the longitudinal plasmon band of the rods.

Introduction

Investigating how size affects the properties of materials is an important area of study in physical science. In the past several years, a number of groups have shown that the quantized acoustic vibrational modes of nanoparticles can be examined by time-resolved laser spectroscopy. These studies have been performed on spherical metal and semiconductor particles (both in solution and with solid supports),[1−7] core−shell bimetallic particles,[8] and Ag ellipses in a glass matrix.[9] In these experiments, an ultrafast laser pulse excites the system and induces rapid expansion. This impulsively excites the phonon mode that correlates to the expansion coordinate of the particles. For spherical particles, the lowest frequency symmetric breathing mode is excited. The measured vibrational frequencies are in excellent agreement with continuum mechanics calculations.[10−12] However, for nonspherical particles the situation is much more complex. In particular, it is not clear which vibrational modes will be excited, and how the frequencies of these modes depend on the size, shape and elastic properties of the material.

In a recent study of aligned ellipsoidal Ag particles in a glass matrix, Perner and co-workers observed a beat signal whose period depended on whether the probe laser was resonant to the longitudinal or transverse plasmon band of the particles.[9] They attributed this signal to expansion and contraction along the major or minor axis of the ellipse. The observed periods are approximately given by $2d/c_l$, where c_l is the longitudinal speed of sound and d is either the length or width of the ellipse. In this paper, we present initial results from our ultrafast laser studies of Au nanorods. The rods were grown by an electrochemical method, and had aspect ratios between 2 and 5 (which

* To whom correspondence should be addressed.
† E-mail: hartland.1@nd.edu.
‡ E-mail: mulvaney@unimelb.edu.au.
§ E-mail: jsader@unimelb.edu.au.

10.1021/jp013887+ CCC: $22.00
Published on Web 01/08/2002

correspond to lengths between 20 and 50 nm). Modulations with a period on the order of 50−70 ps can be clearly seen in our transient absorption data. This period is much longer than that expected from Perner et al.'s results.[9] This difference could arise either because (i) the vibrational mode excited in the nanorods is fundamentally different to the mode excited in the ellipsoidal particles, or (ii) the elastic properties of the Au nanorods cannot be estimated from values for bulk (polycrystalline) Au, due to their inherent crystallinity[13] or small size. The exact value of the period also depends on the probe wavelength, which implies that different wavelengths interrogate different length rods in the sample. The dependence of the measured period on the probe wavelength has been analyzed to obtain information about the homogeneous and inhomogeneous contributions to the extinction spectra of the rods.

Experimental Section

The time-resolved laser experiments were performed with a regeneratively amplified Ti:Sapphire laser. This laser system produces ca. 150 fs pulses at a repetition rate of 1 kHz. The laser fundamental was frequency doubled to give 400 nm pump laser pulses, and tunable probe laser pulses were obtained by generating a white-light continuum in a sapphire window. For a given experiment, the probe laser wavelength was selected with a Jobin−Yvon Spex H-10 monochromator (10 nm spectral resolution) placed after the sample. The pump laser intensity at the sample was ≤ 0.5 μJ/pulse, as measured by a Molectron J3−02 Energy Detector. Based on the measured laser spot size of $\sim 4.5 \times 10^{-4}$ cm^2, this power will produce a temperature rise in the rods of < 200 °C. These temperatures are below the threshold for melting the rods.[14] The sample was held in a 2 mm path length cell, and the experiments were performed without flowing. The pump and probe lasers had parallel polarizations for all the experiments presented below. However, experiments with perpendicular pump and probe polarizations gave identical results (for 400 nm excitation).

The Au nanorods were synthesized by the electrochemical technique first described by Wang and co-workers,[15,16] and were extensively purified to reduce the polydispersity.[17] The dimensions of the rods were analyzed by TEM, using either a Phillips 12 (120 kV) or a Hitachi HF6000 (70 kV) electron microscope. The UV−vis absorption spectra of the samples show the characteristic longitudinal and transverse plasmon resonances, that correspond to oscillation of the conduction electrons along the length or width of the rod. The transverse plasmon band appears at ca. 520 nm for all the samples, whereas the longitudinal resonance depends on the average aspect ratio of the sample.[15,16,18] The nanorods investigated in this work had aspect ratios between 2 and 4.9, which correspond to longitudinal plasmon resonances between 600 and 840 nm. It is important to note that the absorbance at the pump laser wavelength (400 nm) does not depend on aspect ratio, i.e., in our experiments, all the rods in the sample are equally excited by the pump laser pulses.

Results

Figure 1 presents transient absorption data for a gold nanorod sample with an average aspect ratio of 3.5. These experiments were performed with probe laser wavelengths of 650 and 780 nm. These two wavelengths lie on either side of the longitudinal plasmon band of this sample, which occurs at ~720 nm.[17] There are several features to note about the transient absorption data. First, at early times (<20 ps) the signal at 650 nm is a bleach, whereas, the signal at 780 nm is an absorption. Second, both

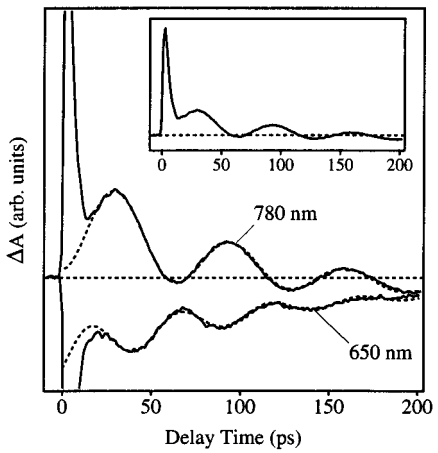

Figure 1. Transient absorption data recorded with 400 nm pump pulses and probe wavelengths of 650 and 780 nm for gold nanorods with an average aspect ratio of 3.5. These two probe laser wavelengths lie on either side of the longitudinal plasmon resonance for this sample.

traces contain an initial decay, which has a time constant of several ps, followed by a slower modulated signal. The initial decay corresponds to cooling of the hot electrons created by the pump laser pulse,[19−21] and the modulations are due to the coherently excited vibrational modes of the rods. The relative magnitude of the modulations compared to the early signal from the hot electrons can be seen in the insert of Figure 1. The coherent vibrational motion is launched by the rapid heating of the electrons and lattice that follows ultrafast laser excitation.[9,22,23]

Both the period and the phase of the modulations are different for the 650 and 780 nm data. Fits to the experimental data using a damped cosine function yield a period and phase of 51 ps and 114° for the 650 nm data, compared to 65 ps and 176° for the 780 nm data. Note that a difference in the phase for transient absorption experiments performed on the red or blue sides of the plasmon band has been previously observed for spherical particles.[5,7,23] However, for spheres the phase difference is 180°, i.e., the modulations are completely out-of-phase. Also note that the period of the modulations is much longer than that expected from Perner et al.'s results. Specifically, from the length of the rods in our sample we would predict a period of $2L/c_l = 22$ ps if the observed modulations were due to expansion and contraction along the long axis of the rod.[9] This is almost a factor of 3 faster than the experimental data in Figure 1.

In Figure 2 the period and phase are plotted against the probe laser wavelength for a series of transient absorption experiments with the same sample as in Figure 1. The period changes from 47 to 75 ps as the probe wavelength is shifted from the blue (600 nm) to the red (860 nm). For spherical particles, the measured period does not change with the probe laser wavelength.[5,23] This difference arises because the longitudinal plasmon resonance of the rods depends on their aspect ratio and, therefore, their length. Thus, different probe wavelengths interrogate different portions of the sample distribution. In contrast, for spherical particles the plasmon band does not shift with size (for particles < 50 nm diameter).[24,25] The relative contributions from different sized spheres in the sample does not change with the probe wavelength, and the main result of polydispersity is to damp the modulations.[23,26] The phase data in Figure 2(b) shows that the coherent response of the sample changes from a sine function for probe wavelengths on the blue side of the longitudinal plasmon band, to a negative cosine function on the red side. In the following discussion, we will

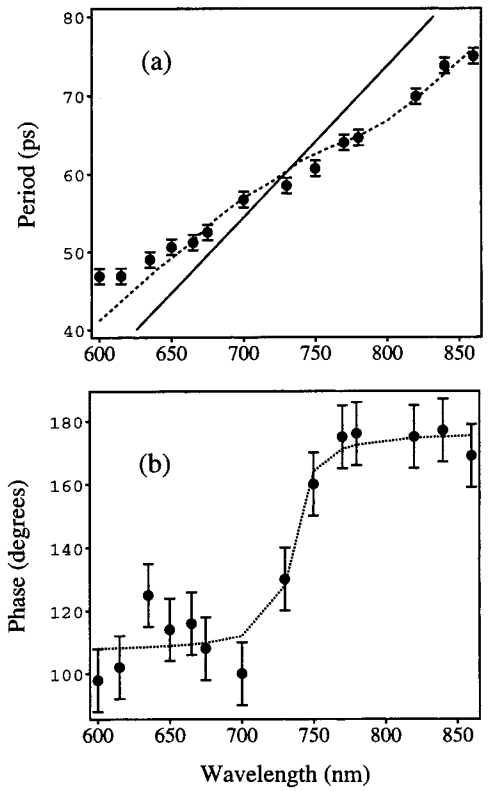

Figure 2. (a) Period of the beat signal versus probe laser wavelength (●) for the 3.5 aspect ratio Au nanorod sample. The solid line shows the period expected from $T = 2L/c_t$ where c_t is the transverse speed of sound in Au. (- - -) Simulations of the period versus probe wavelength data using eqs 3 and 4, see text for details. (b) Phase of the modulations versus probe wavelength for the same sample as in (a). The dashed line is a guide for the eye.

concentrate on the period of the acoustic oscillations, and leave the analysis of the phase to a latter publication.

Discussion

Figure 2(a) shows that the period of the coherently excited vibrational mode increases as the probe laser is tuned to the red. Qualitatively, this occurs because longer probe laser wavelengths interrogate longer rods (on average), and the vibrational period increases with length. For Au nanorods with aspect ratios ≤ 5, the wavelength of the maximum in the longitudinal plasmon band (λ_{max}) is linearly proportional to the aspect ratio of the rod: $\lambda_{max} \approx 86 \times A.R. + 419$.[27] The rods in our samples have a width of ~10 nm, which means that λ_{max} is proportional to L. The approximately linear relationship between the period and probe wavelength therefore suggests that the vibrational period has the form $T = 2L/\alpha$, where α is a constant that depends on the elastic properties of the rods. As noted above, Perner et al. found that for ellipsoidal Ag particles $\alpha = c_l$,[9] in comparison, for our transient absorption experiments we find $\alpha \approx c_t$. In the following analysis, we will assume that the vibrational period for the Au nanorods is given by $2L/c_t$. It is important to remember that this is a purely phenomenological expression.

By using the relationship between λ_{max} and length, the period predicted by $2L/c_t$ can be plotted on the same wavelength scale as the transient absorption data. This is shown as the solid line in Figure 2(a). The experimental values are in reasonable agreement with the calculated periods, but show significant deviation from the predicted linear behavior at high and low wavelengths (i.e., at wavelengths significantly displaced from the longitudinal plasmon resonance). This deviation occurs because of the finite size distribution of the sample. The way a given rod contributes to the signal depends on the overlap of its transient absorption spectrum with the spectrum of the probe laser, and the total signal is the sum of all these contributions.

It has previously been shown that the coherently excited vibrational modes of nanoparticles produce a periodic shift in the position of the plasmon band.[5−8,23] Assuming that the longitudinal plasmon band can be modeled as a Gaussian function, the transient absorption spectrum of a rod of length L, $\Delta A_R(\lambda,t;L)$, can be written as

$$\Delta A_R(\lambda,t;L) = \frac{2(\lambda - \lambda_R(L))}{\sigma_R^2} \times \frac{\exp[-(\lambda - \lambda_R(L))^2/\sigma_R^2]}{\sqrt{\pi}\sigma_R} \times \Delta\lambda_R(t;L) \quad (1)$$

where $\lambda_R(L)$ is the central wavelength of the spectrum, σ_R gives the width of the spectrum, and $\Delta\lambda_R(t;L)$ is the wavelength shift induced by the coherent vibrational motion. The L dependence of $\lambda_R(L)$ and $\Delta\lambda_R(t;L)$ has been explicitly noted. For the present analysis the functional form of $\lambda_R(L)$ is taken to be $\lambda_R(L) = 8.6 \times L + 419$ (i.e., we assume that all the rods have a width of 10 nm). If $W(L)$ is the size distribution function for the rods and $I(\lambda)$ is the probe laser spectrum, then the signal in our experiments is simply

$$S(t) = \int_0^\infty dL \int_0^\infty d\lambda \{W(L) \times I(\lambda) \times \Delta A_R(\lambda,t;L)\} \quad (2)$$

Assuming that $I(\lambda)$ and $W(L)$ are also Gaussian functions, it can be shown that $S(t)$ is given by

$$S(t) = \int_0^\infty dL \left\{ \frac{e^{-(L-\bar{L})^2/\sigma_L^2}}{\sqrt{\pi}\sigma_L} \times \frac{2(\lambda_p - \lambda_R(L))}{\sigma'^2} \times \frac{e^{-(\lambda_p - \lambda_R(L))^2/\sigma'^2}}{\sqrt{\pi}\sigma'} \Delta\lambda_R(t;L) \right\} \quad (3)$$

where $\bar{L}$ and σ_L are the average value and standard deviation of $W(L)$, λ_p is the central wavelength of the probe laser, and $\sigma' = \sqrt{\sigma_R^2 + \sigma_p^2}$ where σ_p and σ_R describe the spectral width of $I(\lambda)$ and $\Delta A_R(\lambda,t;L)$, respectively.

For spherical particles the coherently excited acoustic modes change the position of the plasmon resonance by changing the volume of the particles.[6,8,23] Physically, this occurs because the plasmon resonance depends on the plasma frequency of the metal, which depends on the free electron density. We will assume that this mechanism also applies for the rods.[28] Using the Drude model to calculate the relationship between the electron density and the plasmon resonance yields[24,29]

$$\Delta\lambda_R(t;L) = \frac{\Delta V/V}{2} \lambda_R \times cos[(2\pi/T(L))t + \phi] \quad (4)$$

where $\Delta V/V$ is the volume change induced by the vibrational motion, $T(L) = 2L/c_t$ is the vibrational period, and ϕ is the phase of the beat signal.

The experimental data in Figure 2 was modeled by using eqs 3 and 4 to calculate the signal as a function of time for a given probe laser wavelength. The period was then extracted by fitting the calculated signal to a damped cosine function. The results of these model calculations for a range of probe wavelengths are presented in Figure 2. The parameters used were $\bar{L} = 35$ nm, $\sigma_L = 14$ nm, $\sigma_p = 6$ nm, and $\sigma_R = 40$ nm. Note that the

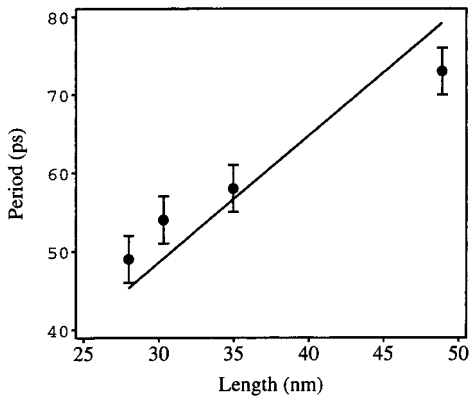

Figure 3. Vibrational period versus length for a series of Au nanorod samples. The periods were evaluated from transient absorption data collected with probe laser wavelengths $\lambda_p \approx \lambda_{max}$. (—) Fit to the data assuming that the period is proportional to the length of the rod.

value of σ_p was determined by the spectral resolution of our detection system, $\bar{L}$ was obtained from TEM analysis of the sample, and σ_L was adjusted to match the calculated and experimental absorbance spectrum. The value of σ_R was then varied to give the best agreement between the calculations and the experimental period versus wavelength data. The results are not particularly sensitive to σ_R, and reasonable fits to the transient absorption data are obtained with $35 < \sigma_R < 55$.

These simple model calculations give a reasonable description of the experimental data. In particular, the calculated period deviates from the straight line predicted by $T(L) = 2L/c_t$ for probe laser wavelengths in the wings of the longitudinal plasmon band. The amount of deviation depends on the width of the absorption spectrum of a single rod (σ_R) compared to the overall width of the longitudinal plasmon band of the sample (which is mainly determined by σ_L, the parameter that describes the polydispersity). Thus, these experiments provide a way of probing the homogeneous line width of the longitudinal plasmon band. The value of σ_R used in the model calculations corresponds to a fwhm = 70 nm for the spectrum of a single rod. This is approximately two times larger than the calculated line widths in ref 18. These calculations were performed using the extended Mie theory developed by Gans[30] and dielectric constant data for bulk gold.[31]

The simulations also show that at probe laser wavelengths near the plasmon band maximum the effect of the sample polydispersity is minimized, i.e., the measured periods are close to the values expected from the average length of the rods. Note that this is true even if the vibrational period does not depend linearly on the rod length. Thus, to compare different samples, the probe laser should be tuned as close to the maximum of the longitudinal plasmon band as possible. Figure 3 shows results for different rod samples, where the period of the acoustic vibrational mode was determined from experiments with $\lambda_p \approx \lambda_{max}$. The straight line is a fit to the data assuming that the period is linearly proportional to the length of the rod, i.e., $T = 2L/\alpha$. The value of α obtained is $\alpha = 1230$ ms^{-1}, which is almost exactly equal to the transverse speed of sound in Au: $c_t = 1200$ ms^{-1}.[32]

At this point, it is not clear why the Au nanorods give a different period compared to the ellipsoidal Ag particles. Two possibilities are as follows: (i) the vibrational modes excited in the Au nanorods are fundamentally different to those for the Ag ellipses (i.e., we are exciting a motion that is much more complicated than simple stretching and compression along a single axis), or (ii) use of materials properties for bulk (polycrystalline) gold is not appropriate for these small crystalline nanorods. This contrasts with the Ag ellipses of ref 9, which are polycrystalline and show good agreement with bulk data. The elastic properties of the single crystal nanorods may be very different to those of polycrystalline rods. Further experiments and detailed continuum mechanics calculations are currently being performed to elucidate the vibrational dynamics of these systems. In addition, we are developing a more sophisticated analysis of the transient absorption spectrum of the rods, to gain more insight into the homogeneous and inhomogeneous contributions to the longitudinal plasmon band.

In summary, ultrafast laser excitation of Au nanorods coherently excites the low frequency acoustic vibrational modes. The measured vibrational periods are proportional to the length of the rods. Due to polydispersity, for a given sample the exact value of the period depends on the probe laser wavelength. Analysis of the period versus wavelength data provides information about the homogeneous line width of the longitudinal plasmon band. The results for a sample with an average length of 35 nm and a width of 10 nm show that the homogeneous line width is approximately two times larger than that calculated from the dielectric constant data for bulk Au.

Acknowledgment. The work described in this paper was supported by the National Science Foundation by Grant No. CHE98-16164 (G.V.H.), and by the Particulate Fluids Processing Centre of the Australian Research Council and the Australian Research Council Grants Scheme (P.M. and J.E.S.). We are grateful to Michael Giersig of the Hahn-Meitner Institut for performing TEM analysis of the samples.

References and Notes

(1) Krauss, T. D.; Wise, F. W. *Phys. Rev. Lett.* **1997**, *79*, 5102.
(2) Nisoli, M.; De Silvestri, S.; Cavalleri, A.; Malvezzi, A. M.; Stella, A.; Lanzani, G.; Cheyssac, P.; Kofman, R.*Phys. Rev. B* **1997**, *55*, R13 424.
(3) Thoen, E. R.; Steinmeyer, G.; Langlois, P.; Ippen, E. P.; Tudury, G. E.; Brito Cruz, C. H.; Barbosa, L. C.; Cesar, C. L. *App. Phys. Lett.* **1998**, *73*, 2149.
(4) Hodak, J. H.; Martini, I.; Hartland, G. V.*J. Chem. Phys.* **1998**, *108*, 9210.
(5) Del Fatti, N.; Voisin, C.; Chevy, F.; Vallée, F.; Flytzanis, C. *J. Chem. Phys.* **1999**, *110*, 11 484.
(6) Hodak, J. H.; Henglein, A.; Hartland, G. V. *J. Chem. Phys.* **1999**, *111*, 8613.
(7) Del Fatti, N.; Voisin, C.; Christofilos, C.; Vallée, F.; Flytzanis, C. *J. Phys. Chem. A* **2000**, *104*, 4321.
(8) Hodak, J. H.; Henglein, A.; Hartland, G. V. *J. Phys. Chem. B*, **2000**, *104*, 5053.
(9) Perner, M.; Gresillon, S.; März, J.; von Plessen, G.; Feldmann, J.; Porstendorfer, J.; Berg, K.-J.; Berg, G. Phys. Rev. Lett. **2000**, *85*, 792
(10) Lamb, H.*Proc. London Math. Soc.* **1882**, *13*, 189.
(11) Dubrovskiy, V. A.; Morochnik, V. S.*Izv. Earth Phys.* **1981**, *17*, 494.
(12) Sader, J. E.; Hartland, G. V.; Mulvaney, P. *J. Phys. Chem. B*, accepted for publication.
(13) Wang Z. L.; Mohamed M. B.; Link S.; El-Sayed M. A. *Surf. Sci.* **1999**, *440*, L809.
(14) Link, S.; El-Sayed, M. A. *J. Chem. Phys.* **2001**, *114*, 2362.
(15) Yu, Y. Y.; Chang, S. S.; Lee, C. L.; Wang, C. R. C. *J. Phys. Chem. B* **1997**, *101*, 6661.
(16) Chang, S. S.; Shih, C. W.; Chen, C. D.; Lai, W. C.; Wang, C. R. C. *Langmuir* **1999**, *15*, 701.
(17) Wilson, O. et al., *Nanoletters*, submitted for publication.
(18) Link, S.; Mohamed, M. B.; El-Sayed, M. A. *J. Phys. Chem. B* **1999**, *103*, 3073.
(19) Hodak, J. H.; Martini, I.; Hartland, G. V. *J. Phys. Chem. B* **1998**, *102*, 6958.
(20) Hodak, J. H.; Henglein, A.; Hartland, G. V. *J. Chem. Phys.* **2000**, *112*, 5942.
(21) Link, S.; Burda, C.; Mohamed, M. B.; Nikoobakht, B.; El-Sayed, M. A. *Phys. Rev. B* **2000**, *61*, 6086.
(22) Voisin, C.; Del Fatti, N.; Christofilos, D.; Vallee, F. *Appl. Surf. Sci.* **2000**, *164*, 131.
(23) Hartland, G. V. *J. Chem. Phys.*, submitted for publication.

(24) Kreibig, U.; Vollmer, M. *Optical Properties of Metal Clusters*, Springer: Berlin, 1995.
(25) Henglein, A.*Langmuir* **1999**, *15*, 6738.
(26) Hodak, J. H.; Henglein, A.; Hartland, G. V. *J. Phys. Chem. B* **2000**, *104*, 9954.
(27) This relationship was determined from the spectra of samples prepared in our laboratory, as well as in refs 15, 16, and 18, and from calculations of the absorption spectra of the rods within the dipole limit.
(28) It is important to note that thermal expansion does not change the aspect ratio of the rods, which means that it does not directly change λ_{max}.
(29) Ashcroft, N. W.; Mermin, N. D. *Solid State Physics*, Harcourt Brace: Orlando, 1976.
(30) Gans, R. *Ann. Physik* **1915**, *47*, 270.
(31) Johnson, P. B.; Christy, R. W. *Phys. Rev. B* **1972**, *6*, 4370.
(32) *CRC Handbook of Chemistry and Physics, 80th ed.* CRC Press: Boca Raton, FL, 1999.